Force-driven polymerization in cells: actin filaments and focal adhesions

2005 J. Phys.: Condens. Matter 17 S3913

(http://iopscience.iop.org/0953-8984/17/47/019)

INSTITUTE OF PHYSICS PUBLISHING JOURNAL OF PHYSICS: CONDENSED MATTER

J. Phys.: Condens. Matter **17** (2005) S3913–S3928 doi:10.1088/0953-8984/17/47/019

Force-driven polymerization in cells: actin filaments and focal adhesions

Tom Shemesh[1], **Alexander D Bershadsky**[2] **and Michael M Kozlov**[1]

[1] Department of Physiology and Pharmacology, Sackler Faculty of Medicine, Tel Aviv University, 69978, Tel Aviv, Israel
[2] Department of Molecular Cell Biology, The Weizmann Institute of Science, Rehovot 76100, Israel

Received 6 September 2005
Published 4 November 2005
Online at stacks.iop.org/JPhysCM/17/S3913

Abstract

We describe a thermodynamic principle determining the phenomenon of protein self-assembly controlled by elastic stresses. This principle is based on the Gibbs–Dühem-like relationship between the chemical potential of the aggregated molecules and the stresses produced by forces acting on a protein aggregate. We present two biological systems whose operation can be driven by this principle: actin filament, a polymerizing processive capping by proteins of the formin family, and focal adhesions mediating a mechanical link between the cytoskeleton and extracellular substrates. We describe the major phenomenology of these systems and overview recent models, aimed at understanding the mechanisms of their functioning.

(Some figures in this article are in colour only in the electronic version)

The functioning of a living being is largely due to a complex muscle system, which enables the generation of forces and the performance of motions. Analogously to highly developed organisms, the life and physiology of elementary biological cells vitally depend on an intracellular system that generates and sustains mechanical forces, and that consists of a cytoskeleton and molecular motors [1, 2]. Mechanical stresses produced by the intracellular force-generating systems largely determine the cell architecture, and underlie such essential biological phenomena as cell spreading and motility, cytokinesis, and transport of intracellular protein and membrane carriers [1]. Understanding the interplay between the cell structure and the intracellular forces is one of the major challenges of cell biology.

Here we address only a small part of this broad complex of problems, and present a thermodynamical consideration of the relationship between the elastic stresses generated within cells and self-assembly of intracellular super-molecular aggregates. Specifically, we consider how the major thermodynamic characteristic, the critical concentration of the self-assembling molecules, is modulated by the elastic stresses. We first present a simple and

fundamental principle underlying the phenomenon of stress-controlled self-assembly, which is based on the Gibbs–Dühem relationship [3] and was first applied to the treatment of intracellular polymers by Hill about two decades ago [4]. We then consider two interrelated classes of intracellular structures, whose assembly–disassembly behaviour, referred to as a mechanosensitive behaviour, has been suggested to be based on this principle [5–7]. The first class comprises focal adhesions (FA) mediating a physical link between the cytoskeleton and the extracellular matrices and substrates [6]. The second class includes complexes of actin filaments with newly discovered proteins called formins [5, 7]. These complexes generate the formation of linear actin bundles that serve as 'railways' for intracellular transport and may play a role in the generation of actin-myosin stress fibres mounting the focal adhesions.

Thermodynamics of force-induced self-assembly. To grasp the essence of the effects of pulling forces on self-assembly, consider an aqueous solution of identical molecules. These molecules exhibit attractive interaction, which can lead to their aggregation into a condensed phase that is able to sustain elastic stresses. The thermodynamic state of the system is determined by the chemical potentials of the molecules in the aggregated and non-aggregated (monomeric) state, denoted respectively by $\mu_{\rm agg}$ and $\mu_{\rm free}$. According to Gibbs thermodynamics, the molecules remain in a monomeric state if $\mu_{\rm free} < \mu_{\rm agg}$. The onset of aggregation requires the chemical potential in the aggregated state to be equal to or smaller than that of the monomers, $\mu_{\rm free} \geqslant \mu_{\rm agg}$.

We assume that, once an aggregate starts forming, pulling forces are applied to its surface and produce elastic stresses within the aggregate (see below for the specific mechanism of force application). Here we will consider only the simplest cases where the inter-aggregate stresses are isotropic. Exact consideration of a general case of anisotropic stresses requires a more involved approach and is beyond the scope of the present review.

The chemical potential of non-aggregated molecules can be presented as

$$\mu_{\rm free} = \mu^0_{\rm free} + \beta \ln \frac{c}{c_{\rm W}}, \tag{1}$$

where c is the molar concentration of monomers in the aqueous solution, $c_{\rm W} \approx 55$ M is the molar concentration of water molecules, $\beta \approx 4 \times 10^{-21}$ J ≈ 0.6 kcal mol^{-1} is a product of the Boltzmann constant and the absolute temperature, and $\mu_{\rm free}$ is the concentration-independent part accounting for the free energy of a monomer interaction with the surrounding medium and referred to below as the standard chemical potential in the monomeric state. The second term in (1) represents the contribution to $\mu_{\rm agg}$ by the entropy of mixing of the monomers in the aqueous solution. Equation (1) is valid for cases of very low concentrations, $c/c_{\rm W} \ll 1$, relevant for intracellular conditions where the protein concentrations are in micromolar ranges.

In the absence of the pulling forces, the chemical potential of the self-assembled molecules that accounts for the interaction between them within the aggregate will be denoted by $\mu^0_{\rm agg}$ and referred to as the standard chemical potential in the aggregated state.

External forces produce elastic stress within the aggregate. The change of the chemical potential of the aggregated molecules, $\mathrm{d}\mu_{\rm agg}$, resulting from the stress change is given by the Gibbs–Dühem-like relationship [3, 8]

$$\mathrm{d}\mu_{\rm agg} = -\frac{\Omega}{N}\,\mathrm{d}T, \tag{2}$$

where N is the number of the aggregated molecules, T represents stress within the aggregate, and Ω is the extensive measure of the aggregate strain conjugated to the stress T. If the aggregate has to be seen as a three-dimensional structure whose surface is subjected to an isotropic normal force, Ω has a meaning of the aggregate volume, $\Omega = V$, and the stress T is a volume tension, having dimensionality of force per unit area $[T] = \mathrm{N\ m^{-2}}$. In the case where

the aggregate can be represented by a surface element subject to an isotropic two-dimensional force, $\Omega = A$ is the surface area, and $T = \sigma$ is a lateral tension with dimensionality of force per unit length $[\sigma] = \mathrm{N\ m^{-1}}$. If the aggregate is a linear polymer whose ends are subject to a pulling or pushing force, $\Omega = L$ is the polymer length, while $T = \gamma$ is a linear tension with dimensionality of force $[\gamma] = N$. Finally, in the case where the aggregate is subject to other types of stress such as shear stress or torsion stress, Ω represents a corresponding extensive variable such as total torsion angle. The value $\frac{\Omega}{N}$ in equation (2) is an intensive value having a meaning of a molecular dimension ω within the aggregate.

To obtain from equation (2) an explicit expression for the chemical potential μ_{agg}, we assume a linear relationship (Hooke law) between the stress T and the molecular dimension ω:

$$T = \kappa \frac{\omega - \omega_0}{\omega_0}, \tag{3}$$

where ω_0 is the molecular dimension at zero tension and κ is the rigidity of the aggregate. The relationship equation (3) is expected to be valid for small deformations,

$$|\omega - \omega_0|/\omega_0 \ll 1. \tag{4}$$

Integration of equation (2) while accounting for equation (3) gives an explicit expression for the chemical potential:

$$\mu_{\mathrm{agg}} = \mu^0_{\mathrm{agg}} - T\omega_0 - \frac{1}{2}\frac{T^2}{\kappa}\omega_0. \tag{5}$$

The two contributions in equation (5) show that a positive stress $T > 0$ produced, for example, by pulling forces acting on the aggregate boundaries reduces the chemical potential of the aggregated molecules μ_{agg}, while a negative stress, $T < 0$, increases μ_{agg}. The relationship presented in equation (5) for the one-dimensional case of a linear polymer has been derived in [4].

We use here the definition of the *critical concentration* c^* as the monomer concentration which is needed for onset of polymerization. (Note that for non-equilibrium polymers such as actin filament, whose constituent monomers hydrolyse ATP in the course of filament growing, the critical concentration in our definition corresponds to a binding constant of monomers to the polymer end. In this case the critical concentration has to be determined separately for each filament end [9].) The critical concentration can be determined from the condition of equality of the chemical potentials, $\mu_{\mathrm{free}} = \mu_{\mathrm{agg}}$, and equations (1) and (5), by

$$c = c^*_0 \exp\left(-\frac{T\omega_0 + \frac{1}{2}\frac{T^2}{\kappa}\omega_0}{\beta}\right) \tag{6}$$

where

$$c^*_0 = c_{\mathrm{W}} \exp\left(\frac{\mu^0_{\mathrm{agg}} - \mu^0_{\mathrm{free}}}{\beta}\right) \tag{7}$$

is the critical concentration in the absence of stresses.

According to equation (6), positive elastic stress, $T > 0$, *decreases* the critical concentration, c^*, hence favouring the molecular self-assembly. A negative elastic stress, $T < 0$, disfavours the aggregation process which is manifested in an *increase* of the critical concentration c^*.

The simple analysis above shows that the elastic stress produced by external forces applied to the aggregate boundaries can control the molecular self-assembly. If the monomer concentration is lower than the critical concentration in the absence of the stresses (equation (7)), $c < c^*_0$, molecules will not self-assemble, or the existing aggregate will undergo

disassembly. After generation of a sufficiently strong stress, according to equation (6), the critical concentration decreases and becomes smaller than the actual monomer concentration, $c > c^*$. As a result, the aggregation process becomes thermodynamically favourable and can be initiated. Once the forces are lifted the formed aggregates will disintegrate again.

In the following we consider two intracellular systems, where the stress-controlled aggregation can play a major role.

1. The role of elastic stresses in actin polymerization upon processive capping by formin

1.1. Actin polymerization and processive capping by formin

Actin polymerization drives fundamental cellular processes such as locomotion, cytokinesis and adhesion. Forces developed as a result of actin polymerization are responsible for different forms of cell motility, and in particular, extension of cell protrusions [9, 10].

Due to an asymmetric structure of actin monomers, an actin filament has a polarity, its two ends having different binding constants for monomeric actin and different polymerization/depolymerization rates [9]. The barbed end (or the plus end) of an actin filament polymerizes faster and has higher binding constants for ATP-actin than the pointed end (or the minus end). Structurally, an actin filament can be described as consisting of two right-handed helical strands of about 71.5 nm pitch distance. Alternatively, the filament structure can be seen as a single left-handed helix with a short pitch of 5.9 nm pitch distance [11–13].

Actin polymerization is tightly regulated by several intracellular proteins, among which the most important are Arp2/3 complex nucleating actin filament polymerization and branching, barbed end capping proteins, which stop actin polymerization at the barbed end; and ADF/cofilin, which promotes actin disassembly by severing the filaments (see, e.g. [14]).

Recently discovered multidomain proteins of the formin family can both nucleate and cap actin filaments [15, 16]. After the nucleation of actin polymerization, formins remain persistently bound to the barbed ends of the growing filaments [17–21] walking with them during the course of polymerization [22]. Due to this property, formins are called 'processive' (or 'leaky') cappers [17], which, in contrast to the usual capping proteins, allow the actin polymerization (and depolymerization) in the barbed direction.

Crystallographic, NMR and biochemical data indicate that a minimal protein module able to perform processive capping is a dimer of the formin homology domain FH2 [23–25]. While being attached to the filament barbed end, an FH2 dimer allows for barbed end polymerization at rates equal to or lower than that of a pure actin filament [17]. Acceleration of the processive capping polymerization requires, in addition to the FH2 dimer, a complex of the formin homology domain FH1 and a profilin protein [18, 21].

FH2 dimer has been suggested to be composed of two structural units, termed actin bridge elements, that form a closed ring-like structure due to reciprocal connections by flexible tethers [24]. It was proposed that the FH2 ring at the barbed end can exist in two configurations, termed closed and open, that differ in the relative position and orientation of the two bridges [24]. In the closed configuration, illustrated in figure 1(a), the barbed end is blocked for addition of new actin monomers, while in the open configuration, one of the bridge elements is available for binding a new actin monomer (figure 1(b)) [24]. Movement of the FH2 ring along the barbed end in the course of transition from the closed to the open state corresponds to the stair-stepping scenario, the term proposed in [25].

Because of the helical structure of the actin filament, the stair-stepping requires the FH2 to rotate relative to the filament [26]. Each stair-stepping step is coupled to rotation of the formin dimer by $\approx 14^\circ$ with respect to the bulk of the filament, in the direction of twist of the

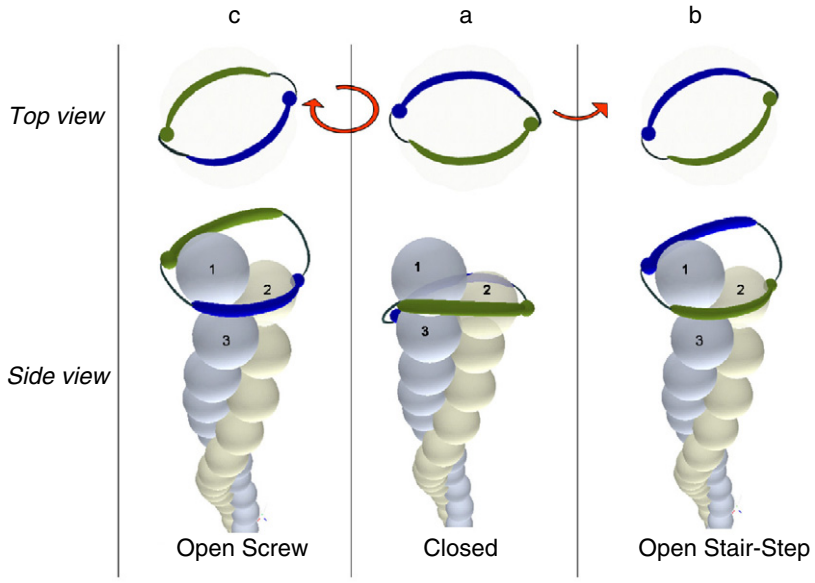

Figure 1. Stair-stepping and screw modes of processive capping. Actin monomers are represented by spheres, and the formin FH2 bridges are shown as blue and green elongated bodies around the filament. Rotation of the orientation of FH2 with respect to the bulk of the filament is represented by red arrows. (a) The closed state, prohibiting insertion of new actin monomers to the filament. Each FH2 bridge binds two actin subunits of the filament end. The green bridge binds the protruding (actin 1) and the penultimate (actin 2) subunits, while the second, blue, bridge binds the actin 2 and actin 3 subunits. (b) The stair-stepping mode of transition from the closed state to an open state capable of actin polymerization. The blue bridge migrates from actins 2 and 3 to actin 1 and exposes its post domain for insertion of a new actin monomer. The direction of rotation of the FH2 dimer in this mode is that of twist of the long-pitch actin helix. The rotation angle is $\sim 14°$. (c) Transition to an open state through the screw mode. The two bridges of FH2 dimer undergo a screw-like motion around the filament until they bind in the new position. The post domain of the green bridge is exposed for insertion of a new actin monomer. The FH2 dimer rotates in the direction of the short-pitch actin helix, which is opposite to the rotation direction of the stair-stepping mode. The rotation angle in the screw mode is $\sim -166°$. Reproduced from *The Journal of Cell Biology* (2005) **170** 889–93 with copyright permission of The Rockerfeller University Press.

long-pitch actin helices (figure 1(b)). A persistent rotation in one direction would be difficult to reconcile with the assembly of cross-linked bundles of actin filaments [26] in budding yeast [27] and from adherent junctions [28]. A continuous turning of the filament ends with respect to the filament bodies, which are interconnected within the bundles, would generate an accumulation of elastic torsion strains and stresses in the system, which would be incompatible with continuous polymerization, and generate filament supercoiling. Attempts to observe a turning of the bulks of polymerizing actin filaments with respect to their formin caps have been undertaken *in vitro* in one-filament experiments where the FH2 cap was attached to the substrate [21]. The experiments revealed neither persistent filament rotation with respect to the substrate, nor filament supercoiling.

The 'rotation paradox' of the stair-stepping scenario of actin polymerization upon processive capping led to a suggestion of another mode of formin behaviour on the barbed end called the screw mode [7]. Within the screw mode, FH2 ring moves along the short-pitch actin helix (figure 1(c)). The twist direction of the short-pitch actin helix is opposite to that of the long-pitch helix [11]. Therefore, rotation of the FH2 dimer in the screw mode is opposite

to that of the stair-stepping mode. The transition from the closed to the open state within the screw mode is coupled to rotation of the FH2 dimer with respect to the bulk of the filament by ≈166° (figure 1(c)) [7].

1.2. Optimal regime of processive capping and the dependence of the critical concentration on torsion stresses

To find the optimal regime of processive capping involving the stair-stepping and screw modes, analysis of elastic torsion deformations of the system has been performed [7]. Here, we present the results of the work [7] in full detail and use them for determination of the interplay between the critical concentration and the elastic stresses accumulated within the filament.

We formulate an elastic torsion model for an actin filament capped at its barbed end by a formin dimer, which is attached by an elastic link to a substrate. We calculate the energy that this system accumulates in the course of polymerization and find the most energetically favourable behaviour of the formin cap in the course of processive capping. Based on determination of the elastic torsion energy, we analyse the changes of the critical concentration.

1.3. Energy of filament torsion

Rotation of formin with respect to the filament pointed end will be referred to as the filament torsion. We propose that in the course of polymerization the formin dimer can behave in either stair-stepping or screw mode. One stair-stepping step of polymerization results in a torsion change of $\phi_{SS} = 14°$, while one screw step leads to a torsion change of $\phi_{SCR} = -166°$. The numbers of the stair-stepping and screw steps will be denoted by n and m, respectively. The torsion angle resulting from unconstrained rotation equals $\phi_S = n\phi_{SS} + m\phi_{SCR}$, and will be referred to as the spontaneous torsion angle. Each polymerization step leads to the filament elongation by $\lambda = 2.75$ nm [12].

We assume that during the first $n_0 + m_0$ steps of polymerization there are no constraints imposed on the relative rotation of the filament ends, so that the accumulated torsion angle, ϕ_0, is equal to its spontaneous value $\phi_0 = \phi_{0S} = n_0\phi_{SS} + m_0\phi_{SCR}$, and the filament length reaches a value $L_0 = (n_0 + m_0)\lambda$. Further polymerization proceeds upon fixation of the filament pointed end and attachment of the formin cap to a substrate (a prototype of such situation is represented by the experimental design of [21]), and, hence, results in accumulation of the elastic stress related to torsion. The next Δn stair-stepping and Δm screw steps generate the torsion angle $\Delta\phi$ and the filament elongation $\Delta L = (\Delta n + \Delta m)\lambda$.

The energy of torsion deformation F_{FIL} of a filament of length L can be presented as

$$F_{FIL} = \frac{1}{2} C L \left(\frac{\phi - \phi_S}{L} \right)^2, \tag{8}$$

where ϕ is the total torsion angle, L is the total filament length and C is the torsion elastic modulus equal to $C \approx 8 \times 10^{-26}$ N m^2 [29]. The difference between the actual torsion angle, ϕ, and its spontaneous value, ϕ_S, represents the torsion strain, $\tau = \phi - \phi_S$. Taking into account that $\phi = \phi_0 + \Delta\phi$, $L = L_0 + \Delta L$, and the above relationships, we obtain for the filament torsion energy

$$F_{FIL} = \frac{1}{2} \frac{C}{\lambda(n_0 + m_0 + \Delta m + \Delta n)} (\Delta\phi - \Delta n\phi_{SS} - \Delta m\phi_{SCR})^2. \tag{9}$$

1.4. Energy of formin cap turning

We further assume that the formin cap, while immobilized on the substrate, can rotate to some extent generating deformation of formin itself and/or of the link connecting formin to the

substrate and/or of the substrate itself. Resistance to such deformation will be characterized by an effective rigidity of the formin–substrate complex, C_L, and its energy F_L expressed as

$$F_L = \tfrac{1}{2} C_L (\Delta\phi)^2. \tag{10}$$

1.5. Total energy of the system

The torsion elastic energy accumulated in the course of processive capping is determined by the number of the stair-stepping steps, n, and screw steps, m. To obtain an expression for the filament torsion energy, we first minimize the total elastic energy, $F_{\mathrm{TOT}} = F_{\mathrm{FIL}} + F_L$ with respect to the torsion angle $\Delta\phi$ accumulated upon restriction of the filament rotation. Using equations (9) and (10), we get the expressions for $\Delta\phi$ and the corresponding torsion strain τ:

$$\Delta\phi = \frac{C}{C + C_L\lambda(n_0 + m_0 + \Delta n + \Delta m)}(\phi_{\mathrm{SS}}\Delta n + \phi_{\mathrm{SCR}}\Delta m) \tag{11a}$$

$$\tau = \frac{C_L\lambda(n_0 + m_0 + \Delta n + \Delta m)}{C + C_L\lambda(n_0 + m_0 + \Delta n + \Delta m)}(\phi_{\mathrm{SS}}\Delta n + \phi_{\mathrm{SCR}}\Delta m). \tag{11b}$$

If the rigidity of the formin–substrate complex vanishes, $C_L \Rightarrow 0$, the angle $\Delta\phi$ is simply an addition to the spontaneous torsion angle accumulated as a result of $\Delta n + \Delta m$ steps of processive capping. In the case of a non-vanishing rigidity $C_L > 0$, the torsion angle $\Delta\phi$ differs from the spontaneous one and leads to building up of an elastic energy.

$$F_{\mathrm{TOT}} = \tfrac{1}{2} C_{\mathrm{EFF}}(\phi_{\mathrm{SS}}\Delta n + \phi_{\mathrm{SCR}}\Delta m)^2, \tag{12}$$

where the effective rigidity of the system, C_{EFF}, is determined by the elastic moduli, C, K_L, and the filament length, $L = \lambda(n + m)$, according to

$$C_{\mathrm{EFF}} = \frac{C_L C}{C + C_L\lambda(n_0 + m_0 + \Delta n + \Delta m)}. \tag{13}$$

If the formin–substrate link is broken, $C_L = 0$, the effective rigidity vanishes, $C_{\mathrm{EFF}} = 0$, and, as expected, the elastic energy is not accumulated for any numbers of steps, n and m. For an infinitely rigid formin–substrate complex, $C_L \Rightarrow \infty$, the effective rigidity is determined only by the torsion elastic modulus C of the actin filament,

$$C_{\mathrm{EFF}} = \frac{C}{\lambda(n_0 + m_0 + \Delta n + \Delta m)}. \tag{14}$$

1.6. Optimal regime of processive capping

The most favourable regime of processive capping corresponds to a minimal accumulation of the elastic energy. Such a regime is determined by an optimal relationship between the number of the stair-stepping, n, and screw, m, steps.

To find the optimal regime of processive capping, we have to determine which of the two modes is most favourable for each step of polymerization. To this end we find the energy cost of one processive capping step, which is performed after the system has undergone $n_0 + \Delta n$ stair-stepping and $m_0 + \Delta m$ screw steps.

Based on equation (12), if the step is performed in the stair-stepping mode, its energy is

$$f_{\mathrm{SS}} = \tfrac{1}{2} C_{\mathrm{EFF}}(2\phi_{\mathrm{SS}}\Delta n + 2\phi_{\mathrm{SCR}}\Delta m + \phi_{\mathrm{SS}})\phi_{\mathrm{SS}}. \tag{15}$$

If the step proceeds in the screw mode, the corresponding energy is

$$f_{\mathrm{SCR}} = \tfrac{1}{2} C_{\mathrm{EFF}}(2\phi_{\mathrm{SS}}\Delta n + 2\phi_{\mathrm{SCR}}\Delta m + \phi_{\mathrm{SCR}})\phi_{\mathrm{SCR}}. \tag{16}$$

The relationship between these energies (equations (15), (16)) determines what kind of step will be most probable. A step of stair-stepping will be performed if $f_{SS} < f_{SCR}$, while in the opposite case of $f_{SS} > f_{SCR}$, a screw step is more favourable.

Let us consider the first step after the beginning of the torsion stress accumulation, meaning $\Delta n = 0, \Delta m = 0$. In this case $f_{SS} = \frac{1}{2}C_{EFF}\phi_{SS}^2$, and $f_{SCR} = \frac{1}{2}C_{EFF}\phi_{SCR}^2$. Because $\phi_{SS} = 14°$, and $\phi_{SCR} = -166°$, we obtain from equations (15), (16) that $f_{SS} < f_{SCR}$, so the first step will be performed in the stair-stepping mode.

Calculation of the energies of the following steps shows that the next several of them will also proceed in the stair-stepping mode. The first screw step comes after Δn^* stair-stepping steps, the condition for this event being $f_{SCR}(\Delta n = \Delta n^*, \Delta m = 0) < f_{SS}(\Delta n = \Delta n^*, \Delta m = 0)$. According to equations (15), (16),

$$\Delta n^* = -\frac{1}{2}\frac{\phi_{SCR} + \phi_{SS}}{\phi_{SS}}. \tag{17}$$

Similar analysis shows that in the course of further polymerization, each screw step happens after a sequence of

$$\Delta n^{**} = -\frac{\phi_{SCR}}{\phi_{SS}} \tag{18}$$

stair-stepping steps.

According to equations (17), (18) and the specific values of ϕ_{SS} and ϕ_{SCR}, the first screw step happens after 5 to 6 steps in the stair-stepping mode, while each other screw step is preceded by 11 to 12 stair-stepping steps.

Summarizing, the optimal regime of continuing processive capping consists of repeating cycles, each of which includes a sequence of 11 to 12 stair-stepping steps followed by one screw step.

1.7. Solution of the 'rotation paradox'

Because the optimal regime of processive capping consists of cycles comprising alternating stair-stepping and screw steps, the torsion angle and the elastic energy of the system change periodically and remain within limited ranges during the whole course of polymerization.

To analyse this issue, we assume that the number of polymerization steps $\Delta n + \Delta m$ performed upon accumulation of torsion stress within the filament–formin is much smaller than the number of the preceding steps, $\Delta n + \Delta m \ll n_0 + m_0$. This assumption does not change the qualitative predictions of our model, but it makes the considerations easier.

Based on equation (11*b*) and equation (18), within the initial cycle and with a good approximation within following cycles of the processive capping the torsion strain changes between $\tau' = -\frac{1}{2}\frac{C_L\lambda(n_0+m_0)}{C+C_L\lambda(n_0+m_0)}(\phi_{SCR} + \phi_{SS})$ and $\tau'' = \frac{1}{2}\frac{C_L\lambda(n_0+m_0)}{C+C_L\lambda(n_0+m_0)}(\phi_{SCR} - \phi_{SS})$. The larger the rigidity of the formin–substrate complex, C_L, the larger is the amplitude of variation of the torsion strain. A maximal amplitude corresponds to $C_L \gg \frac{C}{\lambda(n_0+m_0)}$. In this case, the difference between the maximal and minimal torsion strains constitutes $\tau' - \tau'' = -\phi_{SCR} = 166°$. This means that the torsion strain does not persistently builds up in the course of polymerization, but rather varies within a limit of 166°. The periodic variation of the torsion strain as a function of the number of polymerization steps $\Delta n + \Delta m$ for the case of $C_L \gg \frac{C}{\lambda(n_0+m_0)}$ is illustrated in figure 2(a).

As a consequence of the limited variation of the torsion strain, we predict that processive capping will not result in super-coiling of the actin filament. This is in contrast to what can be expected based on the pure stair-stepping model [21]. Indeed, according to the elastic criterion [30], a filament undergoes super-coiling if its torsion strain exceeds a critical

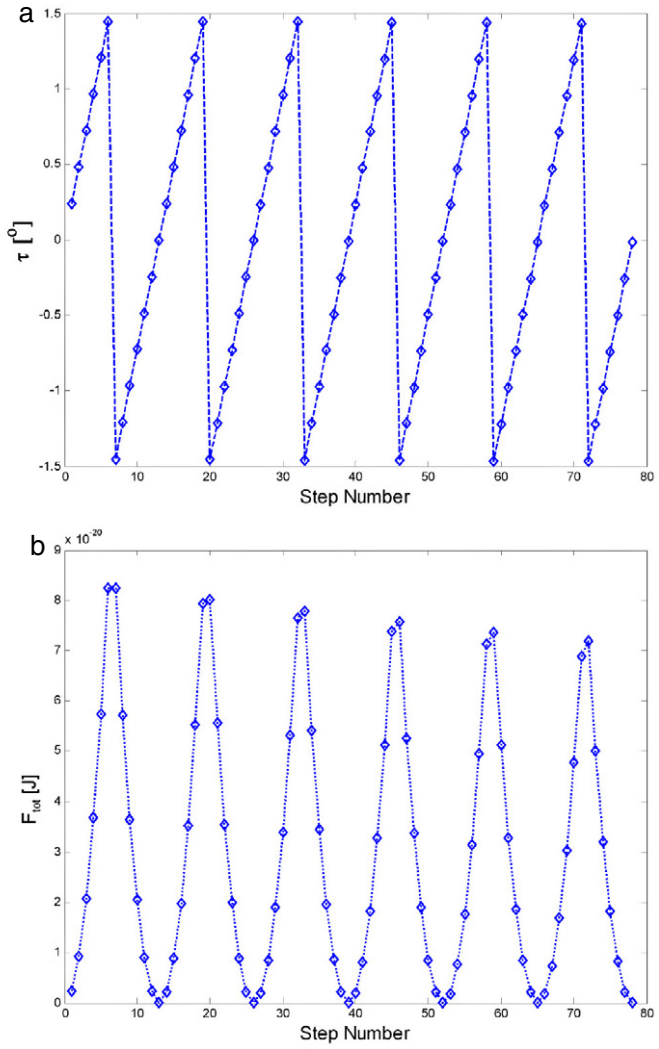

Figure 2. The optimal regime of processive capping consisting of repeated sequences of about 12 stair-stepping steps followed by one screw step. (a) The torsion strain as a function of the number of polymerization steps after the beginning of accumulation of the elastic stresses. The torsion strain changes periodically between the values of $\sim -83°$ and $\sim 83°$. The regions of the positive slope correspond to the stair-stepping mode, while the regions of the negative slope represent the screw mode. (b) Change of the elastic energy in the course of stair-stepping. The elastic parameters used in the calculation are the actin filament torsion modulus $C \approx 8 \times 10^{-26}$ N m^2 [29] and bending modulus $K \approx 3.6 \times 10^{-26}$ J m [31, 32]. It is also assumed that the torsion energy starts to accumulate after the filament reaches a length of 1 μm corresponding to the experimental design of [21]. The energy changes periodically with slowly decreasing amplitude. The maximal energy is reached in the first cycle and does not exceed $\sim 20 k_B T$, where $k_B T \approx 0.6$ kcal M^{-1} is the product of the Boltzmann constant and the absolute temperature. Reproduced from *The Journal of Cell Biology* (2005) **170** 889–93 with copyright permission of The Rockerfeller University Press.

value $\tau^* = \frac{8.98K}{C}$, where K is the filament bending modulus. The bending modulus of an actin filament has a value $K \approx 3.6 \times 10^{-26}$ J m [31, 32], while its torsion rigidity is $C \approx 8 \times 10^{-26}$ J m [29], so the critical torsion equals $\approx 232°$.

Within the optimal regime of processive capping, the maximal absolute value of the torsion strain equals ≈83° (figure 2(a)), which is smaller than the critical value. Hence, the actin filament never reaches the torsion angle generating super-coiling.

The torsion elastic energy F_{TOT} accumulated within the system in the course of polymerization can be determined by combining equations (12) and (18). Variation of the energy in the course of polymerization is illustrated in figure 2(b). Within one cycle of polymerization the torsion energy changes between the values $F_{\mathrm{in}} = \frac{1}{8}\frac{C_L C}{C+C_L\lambda(n_0+m_0)}(\phi_{\mathrm{SCR}} + \phi_{\mathrm{SS}})^2$ and $F_{\mathrm{fin}} = \frac{1}{8}\frac{C_L C}{C+C_L\lambda(n_0+m_0)}(\phi_{\mathrm{SCR}} - \phi_{\mathrm{SS}})^2$. The lower the rigidity C_L of the formin–substrate complex, the smaller is the elastic energy. The largest value of the elastic energy corresponds to the case $C_L \gg \frac{C}{\lambda(n_0+m_0)}$. It is accumulated at the end of the cycle and equals $F_{\mathrm{TOT}}^{\max} = \frac{1}{8}\frac{C}{\lambda(n_0+m_0)}(\phi_{\mathrm{SCR}} - \phi_{\mathrm{SS}})^2$. Assuming that before imposing of the constraint the actin polymers reaches the length of $\lambda(n_0 + m_0) = 1\ \mu$m and using the parameter values $C = 8 \times 10^{-26}$ J m, $\phi_{\mathrm{SCR}} = -166° \approx -2.9$, and $\phi_{\mathrm{SS}} = 14° \approx 0.24$, we obtain for the maximal elastic energy $F_{\mathrm{fin}}^{\max} \approx 20\ k_{\mathrm{B}}T$ (where $k_{\mathrm{B}}T \approx 0.6$ kcal M^{-1} is the product of the Boltzmann constant and the absolute temperature).

Altogether, the cyclic variations of the torsion strain and the corresponding elastic energy (figures 2(a), (b)) within feasible limits demonstrate that the suggested optimal regime of the processive capping combining steps of the stair-stepping and screw modes resolves the 'rotation paradox' of the purely stair-stepping advancement of the formin cap.

1.8. Critical concentration of actin polymerization upon elastic stresses

A formin cap is an ideal molecular device mediating application of external forces to the end of actin filament [5] or transmission of forces exerted by actin polymerization to external objects [21]. Assembly of actin filaments produces forces which are responsible for different forms of cell motility and, in particular, extension of cell protrusions [9, 10]. Force-dependent actin polymerization could underlie such phenomena as stress fibre and focal adhesion formation, driven by myosin II mediated contractility or by externally applied forces [33–36]. According to equation (5), the contribution to the chemical potential of polymerized actin, $\Delta\mu_f$ resulting from a force f acting on the filament ends can be presented as

$$\Delta\mu_f = -f l_0, \tag{19}$$

where $l_0 \approx 2.7$ nm is a change of polymer length resulting from addition of one actin monomer upon the absence of any external force. We have omitted in equation (19) a contribution to $\Delta\mu_f$ proportional to the square of the stress (analogous to the T^2 term in equation (5)) because the ratio of the force f to the stretching rigidity of the actin filament κ is negligibly small. Indeed, while the relevant range of intracellular forces covers the values between several to several tens of pN, κ can be estimated as $\kappa = Ea \approx 1 \times 10^5$ pN, where $E \approx 2 \times 10^9$ N m^{-2} is the Young modulus of polymerized actin [37], and $a \approx 50$ nm^2 is the filament cross-section area [38].

As shown above, formin can also mediate the action of the torsion moment on the filament end. According to equations (15), (16), the change of chemical potential of polymerized actin resulting from one stair-stepping step of polymerization, $\Delta\mu_{\mathrm{SS}}$, is

$$\Delta\mu_{\mathrm{SS}} = \tfrac{1}{2}C_{\mathrm{EFF}}(2\phi_{\mathrm{SS}}\Delta n + 2\phi_{\mathrm{SCR}}\Delta m + \phi_{\mathrm{SS}})\phi_{\mathrm{SS}}, \tag{20}$$

whereas the chemical potential change caused by a screw step of polymerization $\Delta\mu_{\mathrm{SCR}}$ is given by

$$\Delta\mu_{\mathrm{SCR}} = \tfrac{1}{2}C_{\mathrm{EFF}}(2\phi_{\mathrm{SS}}\Delta n + 2\phi_{\mathrm{SCR}}\Delta m + \phi_{\mathrm{SCR}})\phi_{\mathrm{SCR}}. \tag{21}$$

Based on equations (6), (19) the critical concentration in the case where a pulling force acts on the filament end, can be presented as

$$c^* = c_0^* \exp\left(-\frac{f l_0}{\beta}\right). \tag{22}$$

A moderate pulling force of $f \approx 3.5$ pN reduces the critical concentration by an order of magnitude, while a pushing force of the same absolute value results in one order of magnitude increases of c^*.

Variations of the critical concentration produced by the torsion stresses, which are generated in the course of the processive capping, depend exponentially on the changes of the chemical potentials; see equations (20), (21). The critical concentration is not constant in this case, but rather depends on the number of the processive capping step, Δn and Δm. For the stair-stepping steps

$$c_{SS}^*(\Delta n, \Delta m) = c_0^* \exp\left(\frac{1}{2\beta} C_{EFF}(2\phi_{SS}\Delta n + 2\phi_{SCR}\Delta m + \phi_{SS})\phi_{SS}\right), \tag{23}$$

while for the screw steps the critical concentration is

$$c_{SS}^*(\Delta n, \Delta m) = c_0^* \exp\left(\frac{1}{2\beta} C_{EFF}\,(2\phi_{SS}\Delta n + 2\phi_{SCR}\Delta m + \phi_{SCR})\,\phi_{SCR}\right). \tag{24}$$

These results provide a basis for experimental verification of the stair-stepping and screw mechanisms.

2. Role of elastic stresses in self-assembly of focal adhesions

2.1. Phenomenology of focal adhesion mechanosensitivity

Focal adhesions (FAs) are several-micron-large protein complexes, linking the cytoskeleton to the extracellular matrix. An FA consists of a layer of transmembrane integrin molecules and a multi-protein 'sub-membrane plaque'. Integrins are integral membrane hetero-dimeric proteins whose extracellular domains attach to the substrate while their intracellular domains provide docking sites for the assembly of the plaque. The plaque is made up from a wide variety of more than 50 types of different proteins [39]. Stress fibres—bundles of actin filaments, myosin and actin binding proteins—are nucleated and developed at the cytoplasmic end of the focal adhesion, on top of the plaque layer. The stress fibres are major generators of intracellular contractile forces, which are transmitted via the FA plaque and the integrins to the substrate (see the reviews [36, 39, 40]).

While most FAs are stationary structures, in some cases FAs become apparently mobile and start crawling along the substrate in the direction of the force applied by the stress fibres [41–45]. It should be emphasized that, at the molecular level, both stationary and mobile FAs are dynamic structures undergoing a continuous exchange of components with the diffusible cytoplasmic pool, as evidenced by FRAP experiments [46, 47].

Mechanosensitivity of focal adhesions is manifested in the dependence of their shapes and dimensions on the applied forces [35, 36, 48]. A developing FA usually acquires an elongated shape with a finite length, determined by the direction of force and its magnitude. In most cases the size of focal adhesions is proportional to the applied force [49].

The force-induced FA elongation is a reversible process. Impairment of the myosin contractile activity by chemical or natural (e.g. caldesmon) acto-myosin inhibitors, reduces the pulling forces and leads to shrinkage of the FAs (see the review [40]).

FA mechanosensitive behaviour is proved to be largely independent of the origin of the pulling forces, as is seen when the actin–myosin contractile stresses are replaced by external

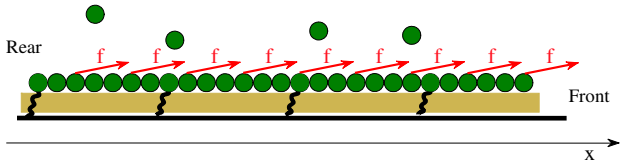

Figure 3. One-dimensional aggregate subject to pulling forces, f (red arrows), and anchored to substrate: illustration of the model. The points of force application and the points of anchoring are distributed along the aggregate surface, each with its own density. Reproduced from *Proc. Natl Acad. Sci.* 2005 **102** 12383–88 with permission.

forces applied either using a micropipette attached to the cell surface or via flexible substrates. Such externally applied forces result in FA dynamics similar to that occurring under natural conditions [48]. Finally, it is noteworthy that the force dependent growth of FAs is due to protein self-assembly. This has been demonstrated by experiments showing a net addition of new fluorescently labelled plaque proteins to the growing, stressed FAs [48, 49].

2.2. Modelling focal adhesions

A model for focal adhesions has been developed in [6], and its major results are presented here. As shown above, the force-induced incorporation of new building blocks into the aggregate proceeds unidirectionally. Therefore, to account for the major features of the system we consider a one-dimensional aggregate consisting of identical molecules. The aggregate is anchored to the substrate by links and is subjected to forces pulling along the aggregate axis (figure 3). To describe the positions along the aggregate we choose the axis x originating at the aggregate rear and directed towards its front (figure 3). The aggregate length will be denoted by L.

We assume that the molecular exchange between the aggregate and the surrounding medium can occur at every point along the aggregate length. Whereas the current data do not provide an unambiguous support for this assumption, the rapid FRAP of paxilin [50] and motion of vinculin within FAs [51] demonstrate that at least for the plaque proteins our assumption is plausible.

In our model, the pulling forces are applied to the aggregate in discrete points. The value of the force in each of such points, referred to below as the elementary force, is denoted by f. One of the points of force application is located at the front edge of the aggregate ($x = L$), while the others are distributed along the aggregate with a constant linear density ϕ_f (figure 3).

The anchors are distributed along the aggregate with linear density ϕ_A and one of the anchors is situated at the rear edge ($x = 0$) (figure 3).

Because of the distribution of the points of force application and the anchors along the aggregate length, the stress $\gamma(x)$ generated within the aggregate depends on the position within the aggregate indicated by x. As a result, the critical concentration is also different for different sections of the aggregate:

$$c^*(x) = c_0^* \exp\left(-\frac{\gamma(x) l_0}{\beta}\right). \tag{25}$$

The molecular exchange between the aggregate and cytosol is determined by the relationship between the concentration, c, and the critical concentration, $\Delta c = c - c^*(x)$ which set the flux $J \sim \Delta c$ of molecules towards the aggregate.

The non-assembled molecules tend to join the aggregate if $Jc > 0$, and leave the aggregate if $Jc < 0$.

Analysis of this model of focal adhesions [6] has shown that, depending on the system parameters, different regimes of self-assembly are possible. The major parameter determining the system behaviour is a ratio between the elementary pulling force multiplied by the molecular length and the difference of the standard chemical potentials:

$$\chi = \frac{f l_0}{\Delta\mu^0}. \tag{26}$$

There can be four different regimes of self-assembly, whose criteria are determined by two characteristic values of the parameter χ:

$$\chi = 1, \qquad \text{and} \qquad \chi = \chi^* = \frac{2\phi_A}{\phi_A + \phi_f}. \tag{27}$$

The two extreme regimes are an unlimited growth and unrestricted disintegration of the aggregate. They correspond, respectively, to small and large values of the elementary force, f, and, hence, also of the parameter χ (equation (26)).

(1) If χ is smaller than the both critical values equation (27),

$$\chi < 1, \qquad \text{and} \qquad \chi < \chi^*, \tag{28}$$

the total flux J is negative for any value of the aggregate length L, as illustrated in figure 4(a). This means that the aggregate does not start to self-assemble. Alternatively, if the force was initially large but has been dropped to a small value satisfying equation (28), the aggregate disintegrates.

(2) If χ is larger than the two critical values,

$$\chi > 1, \qquad \text{and} \qquad \chi > \chi^*, \tag{29}$$

the total flux J is positive for any length (figure 4(b)) and the aggregate undergoes unlimited growth.

The two other regimes correspond to intermediate values of the pulling force f.

(3) If the parameter χ satisfies

$$\chi < 1, \qquad \text{but } \chi > \chi^*, \tag{30}$$

the total flux is negative for the aggregate length smaller than a certain value L^*, but becomes positive for $L > L^*$, as illustrated in figure 4(c). This means that the aggregate does not self-assemble spontaneously for small lengths, but once it achieves the length L^*, due to fluctuations or some unaccounted additional factors, the force-induced self-assembly takes over and the aggregate starts to grow unlimitedly. This regime is possible if the density of the anchors is smaller than that of the points of force application, $\phi_A < \phi_f$.

(4) The final possible regime occurs when

$$\chi > 1, \qquad \text{but, at the same time } \chi < \chi^*, \tag{31}$$

the total flux J is positive for the small lengths L of the aggregate, meaning that the pulling force initiates self-assembly. However, when the length reaches a particular value L_{st}, the flux vanishes and for $L > L_{\mathrm{st}}$ becomes negative (figure 4(d)). This means that the aggregate reaches a finite length $L = L_{\mathrm{st}}$ and stops growing. Hence, L_{st} is the finite steady-state length. Moreover, as follows from (figure 4(d)), this steady state is stable.

A finite steady-state length of the aggregate is possible if the density of the anchors exceeds that of the points of force application, $\phi_A > \phi_f$. In this case, the steady-state length is given by

$$L_{\mathrm{st}} = \frac{2}{(\phi_f + \phi_A)} \frac{(\chi - 1)}{(\chi^* - \chi)}. \tag{32}$$

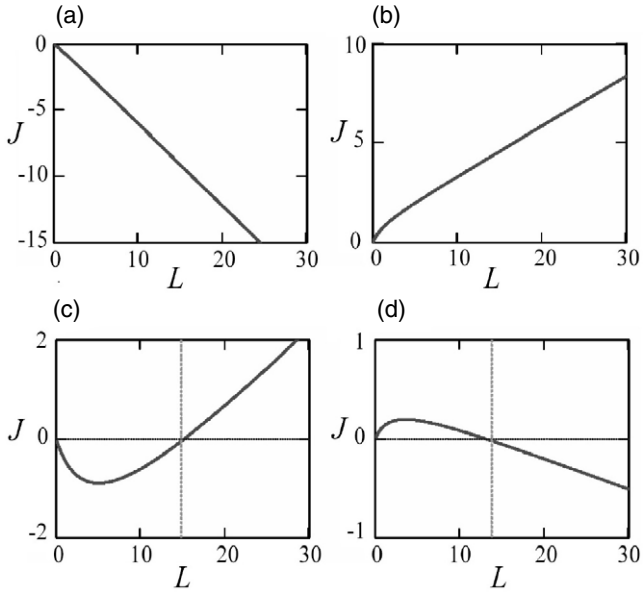

Figure 4. The total flux into the aggregate as a function of the aggregate length, L, in four different self-assembly regimes, determined by the value of the dimensionless parameter $\chi = \frac{fl_0}{\Delta\mu^0}$. (a) At $\chi < 1$, and $\chi < \chi^*$ negative flux for all values of the length, meaning that the aggregate always undergoes disintegration. (b) At $\chi > 1$, and $\chi > \chi^*$ positive flux at every length, meaning that the aggregate undergoes unlimited growth. (c) At $\chi < 1$ but $\chi > \chi^*$ the flux is negative until the aggregate reaches a certain length where the flux changes sign and starts increasing with the aggregate length. This regime corresponds to unlimited growth after overcoming a critical length. (d) At $\chi > 1$, and $\chi < \chi^*$ the flux remains positive until the aggregate reaches a critical length. For lengths larger than the critical values, the flux is negative. This corresponds to a steady-state size of the aggregate. Reproduced from *Proc. Natl Acad. Sci.* 2005 **102** 12383–88 with permission.

According to equation (32), the steady-state length starts from zero at $\chi = 1$ and increases to infinitely large values at χ approaching χ^*.

The four possible regimes and the corresponding ranges of the parameters can be presented as a phase diagram (figure 5).

All four regimes illustrated by the phase diagram (figure 5) have been observed in live cell experiments (see the review [36]). A stationary FA self-assembles, and reaches a finite size as long as pulling forces are acting on its surface. A decrease of pulling results in reduction of the FA size [49]. Complete blockage of the pulling forces acting of the FA leads to its disassembly [52, 53]. Also the mobile FAs have been shown to exhibit growing, shrinking or a constant length in the course of their movement with respect to the substrate [41, 43, 44]. Hence, the mechanosensitive behaviour of stationary and mobile FAs can be understood based on a thermodynamic principle, according to which self-assembly can be driven by the stresses generated within an FA by pulling forces.

3. Conclusions

The aim of this review is to show that, according to general thermodynamics, elastic stresses can determine the regime of molecular self-assembly, and that this phenomenon can be relevant for intracellular processes. The examples of actin filament polymerization upon processive

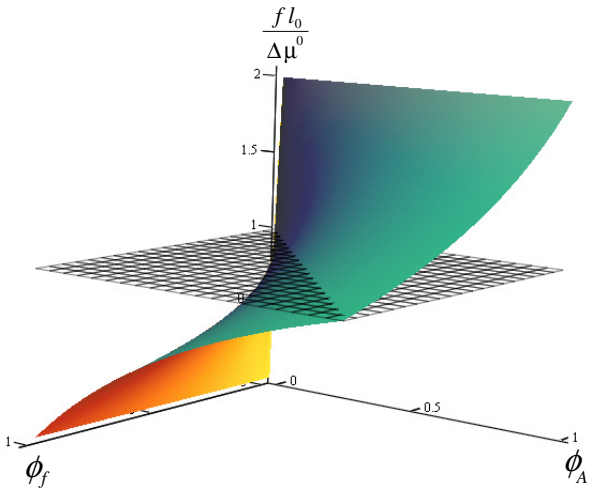

Figure 5. Phase diagram showing the different regimes of FA assembly–disassembly as a function of the system parameters: the density of the points of force application along the aggregate length, ϕ_f, the density of the points of the aggregate anchoring to the substrate, ϕ_A, and the dimensionless parameter $\chi = \frac{f l_0}{\Delta\mu_0}$. Reproduced from *Proc. Natl Acad. Sci.* 2005 **102** 12383–88 with permission.

capping by formin and of mechanosensitive behaviour of focal adhesions demonstrate that the stresses developed between cytoskeletal elements are sufficiently strong to considerably change the critical concentration of aggregation and, hence, to modulate the process of self-assembly. We believe that the suggested non-specific thermodynamic mechanism provides a background for mechanosensitivity of intracellular systems, while specific signalling mechanisms serve for time and space modulation of molecular self-assembly adapting it to various biological requirements.

References

[1] Alberts B *et al* 2002 *Molecular Biology of the Cell* (New York: Garland)
[2] Howard J 2001 *Mechanics of Motor Proteins and the Cytoskeleton* (Sunderland: Sinauer)
[3] Gibbs J W 1961 *The Scientific Papers* (New York: Dover)
[4] Hill T L 1987 *Linear Aggregation Theory in Cell Biology* (New York: Springer)
[5] Kozlov M M and Bershadsky A D 2004 *J. Cell Biol.* **167** 1011
[6] Shemesh T *et al* 2005 *Proc. Natl Acad. Sci. USA* **102** 12383
[7] Shemesh T *et al* 2005 *J. Cell Biol.* **170** 889
[8] Reif F 1965 *Fundamentals of Statistical and Thermal Physics* (New York: McGraw-Hill)
[9] Pollard T D and Borisy G G 2003 *Cell* **112** 453
[10] Mogilner A and Oster G 2003 *Curr. Biol.* **13** R721
[11] Holmes K C *et al* 1990 *Nature* **347** 44
[12] Lorenz M, Popp D and Holmes K C 1993 *J. Mol. Biol.* **234** 826
[13] Steinmetz M O *et al* 1997 *J. Struct. Biol.* **119** 295
[14] Pollard T D 2004 *Cell Motility* ed A Ridley, M Peckham and P Clark (New York: Wiley)
[15] Zigmond S H 2004 *Curr. Opin. Cell Biol.* **16** 99
[16] Wallar B J and Alberts A S 2003 *Trends Cell Biol.* **13** 435
[17] Zigmond S H *et al* 2003 *Curr. Biol.* **13** 1820
[18] Romero S *et al* 2004 *Cell* **119** 419
[19] Pruyne D *et al* 2002 *Science* **297** 612

[20] Pring M *et al* 2003 *Biochemistry* **42** 486
[21] Kovar D R and Pollard T D 2004 *Proc. Natl Acad. Sci. USA* **101** 14725
[22] Higashida C *et al* 2004 *Science* **303** 2007
[23] Li F and Higgs H N 2003 *Curr. Biol.* **13** 1335
[24] Otomo T *et al* 2005 *Nature* **433** 488
[25] Xu Y *et al* 2004 *Cell* **116** 711
[26] Pollard T D 2004 *Dev. Cell* **6** 312
[27] Yang H C and Pon L A 2002 *Proc. Natl Acad. Sci. USA* **99** 751
[28] Kobielak A, Pasolli H A and Fuchs E 2004 *Nat. Cell Biol.* **6** 21
[29] Tsuda Y *et al* 1996 *Proc. Natl Acad. Sci. USA* **93** 12937
[30] Landau L D and Lifshitz E M 1959 *Fluid Mechanics* (Oxford: Pergamon)
[31] Gittes F *et al* 1993 *J. Cell Biol.* **120** 923
[32] Isambert H *et al* 1995 *J. Biol. Chem.* **270** 11437
[33] Burridge K and Chrzanowska-Wodnicka M 1996 *Annu. Rev. Cell Dev. Biol.* **12** 463
[34] Galbraith C G and Sheetz M P 1998 *Curr. Opin. Cell Biol.* **10** 566
[35] Geiger B and Bershadsky A 2002 *Cell* **110** 139
[36] Bershadsky A D, Balaban N Q and Geiger B 2003 *Annu. Rev. Cell Dev. Biol.* **19** 677
[37] Kojima H, Ishijima A and Yanagida T 1994 *Proc. Natl Acad. Sci. USA* **91** 12962
[38] Huxley H E *et al* 1994 *Biophys. J.* **67** 2411
[39] Zamir E and Geiger B 2001 *J. Cell Sci.* **114** 3583
[40] Geiger B and Bershadsky A 2001 *Curr. Opin. Cell Biol.* **13** 584
[41] Zamir E *et al* 2000 *Nat. Cell Biol.* **2** 191
[42] Wehrle-Haller B and Imhof B 2002 *Trends Cell Biol.* **12** 382
[43] Smilenov L B *et al* 1999 *Science* **286** 1172
[44] Small J V and Kaverina I 2003 *Curr. Opin. Cell Biol.* **15** 40
[45] Webb D J, Parsons J T and Horwitz A F 2002 *Nat. Cell Biol.* **4** E97
[46] Tsuruta D *et al* 2002 *Faseb. J.* **16** 866
[47] Ballestrem C *et al* 2001 *J. Cell Biol.* **155** 1319
[48] Riveline D *et al* 2001 *J. Cell Biol.* **153** 1175
[49] Balaban N Q *et al* 2001 *Nat. Cell Biol.* **3** 466
[50] von Wichert G *et al* 2003 *EMBO J.* **22** 5023
[51] Hu K *et al* 2004 *Mol. Biol. Cell* **15** (Suppl.) 177a
[52] Helfman D M *et al* 1999 *Mol. Biol. Cell* **10** 3097
[53] Chrzanowska-Wodnicka M and Burridge K 1996 *J. Cell Biol.* **133** 1403